Numerical Ways to Characterize the Deterioration of Nanofiltration Membranes

S. Déon[1,*], P. Dutournié[2], L. Limousy[2], P. Bourseau[3] and P. Fievet[1]

[1]*Institut UTINAM (UMR CNRS 6213), Université de Franche-Comté, 16 route de Gray, 25030 Besançon Cedex, France*

[2]*IS2M (UMR CNRS 7361), Université de Haute-Alsace, 3 bis rue A. Werner, 68093 Mulhouse Cedex, France*

[3]*Laboratoire GEPEA (UMR CNRS 6144), Université de Bretagne Sud, rue de Saint-Maudé, 56321 Lorient Cedex, France*

Abstract: In this study, a transport model is used to characterize structural and physico-chemical changes in a nanofiltration membrane during the filtration of ionic mixtures. The membrane state is analyzed by a set of four model parameters identified from glucose and salts filtration: the membrane water permeability (L_p), the mean pore radius (r_p), the membrane charge density (X_d), and the dielectric constant of the solution inside pores (ε_p). The study of these structural and physico-chemical properties allows us to determine if deterioration or fouling occurred during filtration. Two distinct identification procedures from filtration of synthetic solutions are investigated in this paper. One is based on the filtration of single salt solutions, whereas the other lies in parameters identification from mixtures containing at least three ions. These methods are applied here to characterize influence of fouling deposit formation and membrane cleaning.

Keywords: Nanofiltration, Transport model, Membrane characterization, Fouling.

INTRODUCTION

Nanofiltration is a recently developed membrane process, which has many applications for industrial and environmental aspects. Indeed, it exhibits many advantages compared to other processes because of its easy process control, lower energy consumption, and its environmental respect, *i.e.* it does not require chemical addition. Salt rejection by nanofiltration membranes is governed by steric, electrostatic as well as dielectric effects, which allow the separation between small or weakly charged ions and bigger or more charged species. For this reason, nanofiltration is a perfectly suitable process for charged solutes fractionation and a very competitive process for industrial and environmental purposes, such as brackish and seawater desalination [1, 2], production of drinking water [3], recovery of high-value solutes [4, 5], or wastewater decontamination [6, 7].

In the last decades, many authors have studied the transfer of ionic compounds through nanofiltration membranes [8, 9]. Indeed, a knowledge model can help to understand the physical mechanisms acting on ions transfer through the membrane but also how these phenomena govern the selectivity towards various ions. This fundamental approach aims at elaborating a simulation tool to predict ionic separation performances of nanofiltration membranes. In this context, the present paper deals with the use of such a model as a tool for the follow-up of membrane state through the identification of the four model parameters.

This paper starts with a short physical description of the model. Next, the proposed methods for parameters identification will be presented in the case of single salt solutions (NaCl) or binary mixtures (NaCl-$MgCl_2$). Various filtration results carried out in identical operating conditions (salt nature, concentrations, and hydrodynamic conditions) will be presented for a same membrane in various states, *i.e.* clean, fouled or chemically regenerated. Parameters obtained in these various membrane states will be thus presented and discussed to show the usefulness of a knowledge model in membrane processes.

THEORETICAL PART

The model used in this study is called Pore Transport Model (PTM). It was accurately detailed in a previous paper [10]. Within the framework of the PTM, modeling is focused on the transport within pores and the transfer through membrane-solution interfaces. Transport through the concentration polarization layer, which was found to strongly influence rejection performances [11], is not modeled but its contribution is taken into account by calculating real rejection $R_{i,m}$ from experimental observed rejection $R_{i,obs}$. This estimation is carried out with the so-called "Velocity Variation Method" (VVM), which is briefly presented in the "Material and Methods" section.

*Address correspondence to this author at the Institut UTINAM (UMR CNRS 6213), Université de Franche-Comté, 16 route de Gray, 25030 Besançon Cedex, France; Tel: (33) 3 63 08 25 81; Fax: (33) 3 81 66 62 88;
E-mail: sebastien.deon@univ-fcomte.fr

The ion transport through the membrane is described as a one-dimensional transport in cylindrical nanometer-sized pores under laminar flow conditions. Ion fluxes are calculated by the extended Nernst-Planck equation, which describes flux as a result of diffusion, convection and electro migration contributions, corrected to take account of pore size [12]:

$$j_i = -K_{i,d} D_{i,\infty} \frac{dc_i}{dx} - \frac{z_i c_i K_{i,d} D_{i,\infty}}{RT} F \frac{d\psi}{dx} + K_{i,c} c_i V \quad (1)$$

with c_i and $D_{i,\infty}$ the concentrations in pores and the infinite diffusivity of an ion i, respectively. V is the solvent velocity within the pore, which is calculated with the Hagen-Poiseuille expression.

Introducing $j_i = V C_{i,p}$ in Eq. 1 yields to:

$$\frac{dc_i}{dx} = \frac{V}{K_{i,d} D_{i,\infty}} \left(K_{i,c} c_i - C_{i,p} \right) - \frac{z_i c_i}{RT} F \frac{d\psi}{dx} \quad (2)$$

Derivation of the electroneutrality equation within the pore with respect to x and introduction of Eq. 2 lead to the expression of the electrical potential gradient $d\psi/dx$:

$$\frac{d\psi}{dx} = \frac{\sum_{i=1}^{n} \frac{z_i V}{K_{i,d} D_{i,\infty}} \left(K_{i,c} c_i - C_{i,p} \right)}{\frac{F}{RT} \sum_{i=1}^{n} z_i^2 c_i} \quad (3)$$

The equilibrium partitioning at the interfaces between pore and bulk solutions are computed from the so-called Donnan Equilibrium improved to take account of molecular interactions as well as steric and dielectric exclusions [8]:

$$\frac{c_i}{C_i} = \frac{\gamma_{i,sol}}{\gamma_{i,pore}} \phi_i \exp\left(-\Delta W_i\right) \exp\left(\frac{-z_i F}{RT} \Delta\psi_D \right) = \phi' \exp\left(\frac{-z_i F}{RT} \Delta\psi_D \right) \quad (4)$$

where $\gamma_{i,sol}$ and $\gamma_{i,pore}$, the activity coefficients, respectively of the bulk solution and of the solution within the pores, are calculated with the extended Debye-Hückel relation. $\Delta\psi_D$ is the so-called Donnan potential and ΔW_i is the solvation energy barrier which can be represented by a decrease of the effective dielectric constant of the solution in the pores as described by the Born model (Eq. 7). ϕ' is a coefficient including the influences of activity coefficients ratio, and steric and dielectric effects.

The concentration of a given ion at the pore inlet is obtained by equaling the Donnan potential, which is the same for each ion, and introducing the so-obtained relations in the electroneutrality equation:

$$z_1 c_1(0) + \sum_{2}^{n} \left[z_i \phi'_i C_{i,m} \left(\frac{c_1(0)}{\phi'_1 C_{1,m}} \right)^{z_i / z_1} \right] + X_d = 0 \quad (5)$$

Concentrations of the other ions are calculated by the relation:

$$\left(\frac{c_i(0)}{\phi'_i C_{i,m}} \right)^{1/z_i} = \left(\frac{c_j(0)}{\phi'_j C_{j,m}} \right)^{1/z_j} \quad (6)$$

The dielectric effects describe the solvation energy decrease of the solvent within the pores. This decrease leads to a solvation energy barrier at the interfaces, which is computed in the model by the Born model [13]:

$$\Delta W_i = \frac{z_i^2 e^2}{8\pi\varepsilon_0 k T r_i} \left(\frac{1}{\varepsilon_p} - \frac{1}{\varepsilon_s} \right) \quad (7)$$

It should be mentioned that the influence of "image forces" [14] on the solvation energy barrier is not neglected but only taken account through a decrease of the effective dielectric constant ε_p, which includes all the phenomena acting on the solvation energy (*i.e.* "image forces", confinement, electrical field, physico-chemical environment,…).

The volumetric permeation flux is calculated from:

$$J_v = \frac{L_p}{\eta} \left(\Delta P - \Delta\pi \right) \quad (8)$$

where L_p is the hydraulic permeability, η the dynamic viscosity of the solution, ΔP the applied pressure and $\Delta\pi$ the osmotic pressure difference calculated with the Van't Hoff relation.

Membrane characterization and performances prediction require the identification of the four model input parameters:

- The water permeability L_p and the mean pore radius r_p, which give hydrodynamic information on the membrane state
- The (effective) dielectric constant within the pores ε_p and the membrane charge density X_d, which provide information on the water confinement inside pores and the electric properties of the membrane, respectively.

MATERIAL AND METHODS

Experiments were carried out with a semi-industrial pilot plant (depicted in Figure **1**). This setup is equipped

with an AFC40 tubular polyamide film membrane (d = 12.7 mm, L = 1.22 m) supplied by PCI Membrane Systems Ltd (Basingstoke, UK). Four cross-flow rates were studied, varying from 500 to 2000 L/hr (*i.e*. velocities from 1.3 to 3.4 m/s) and 6 pressures varying from 8 to 28 bars. Temperature in the plant was held constant at 25°C through circulation in a counter-current heat exchanger cooled by a refrigerating unit. Concentrations were kept constant by recycling permeate into the feeding tank except during flow rate measurements and sampling for concentration analyses. Water flux measurements, cleaning and salt solutions preparation were performed using demineralized water with a residual conductivity lower than 0.1 µS/cm. All experiments were carried out at the native pH of demineralized water, *i.e*. close to 6.

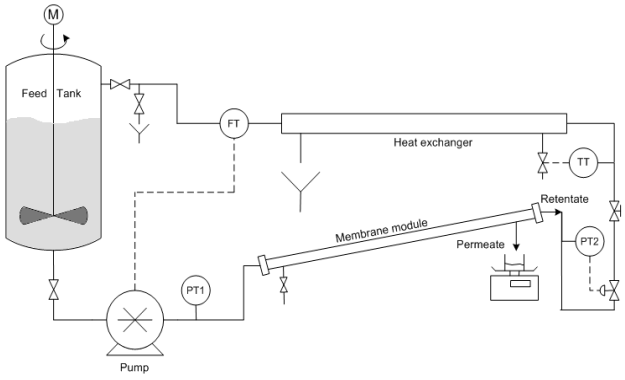

Figure 1: Experimental filtration setup.

The mean pore radius was estimated through the filtration of glucose solutions. These solutions were analyzed by an enzymatic colorimetric method using a reagent GOD-PAP kit coupled with a UV/visible spectrometer.

Ions concentrations in permeate and retentate streams were measured by an ionic chromatography apparatus (ICS 1000, Dionex, Voisins le Bretonneux, France) equipped with a conductivity detector for the measurements of ion concentrations.

For each experiment, the real rejection $R_{i,m}$ curves were determined from observed rejection $R_{i,obs}$ by the Velocity Variation Method (VVM) [15] to overcome the concentration polarization phenomenon.

$$\ln\left(\frac{1-R_{i,obs}}{R_{i,obs}}\right)=\ln\left(\frac{1-R_{i,m}}{R_{i,m}}\right)+\frac{J_v}{k} \quad (9)$$

$$\text{with } R_{i,obs}=1-\frac{C_{i,p}}{C_{i,r}} \quad (10)$$

$$R_{i,m}=1-\frac{C_{i,p}}{C_{i,w}} \quad (11)$$

J_v is the permeation flux, k the mass transfer coefficient and $C_{i,p}$ the concentration of the permeate stream. The VVM consists in determining the observed rejection $R_{i,obs}$ for various increasing tangential velocities, and extrapolating these values to an infinite velocity. The limit value ($R_{i,m}$) thus corresponds to a virtual situation where no polarization layer exists (*i.e*. concentration at the membrane wall $C_{i,w}$ equals to that of the bulk solution $C_{i,b}$):

$$R_{i,m}=\lim_{U_t\to\infty} R_{obs}(U_t) \quad (12)$$

An example of the determination of real rejection curves is illustrated for a NaCl solution in Figure **2**.

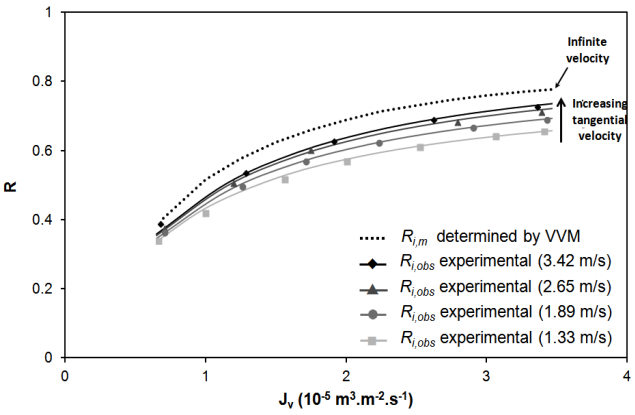

Figure 2: Determination of the real rejection curve of NaCl 10^{-2} M from observed rejection curves at four tangential velocities.

In a first step, a membrane fouling was developed naturally during filtration assays of ionic solutions. It is worthwhile to mention that only synthetic solutions made with demineralized water were filtered during this study, so that fouling was assumed to be due to a biofilm development. This biofilm was detected because permeation flux strongly decreased during experiments. It was thus possible to characterize the membrane state before and after biofilm development as well as after a chemical cleaning.

In a second time, membrane was stored after cleaning during one year in order to obtain a biofilm similar to that observed during filtration experiments of single NaCl solutions. Filtration assays were carried out before and after this storage period.

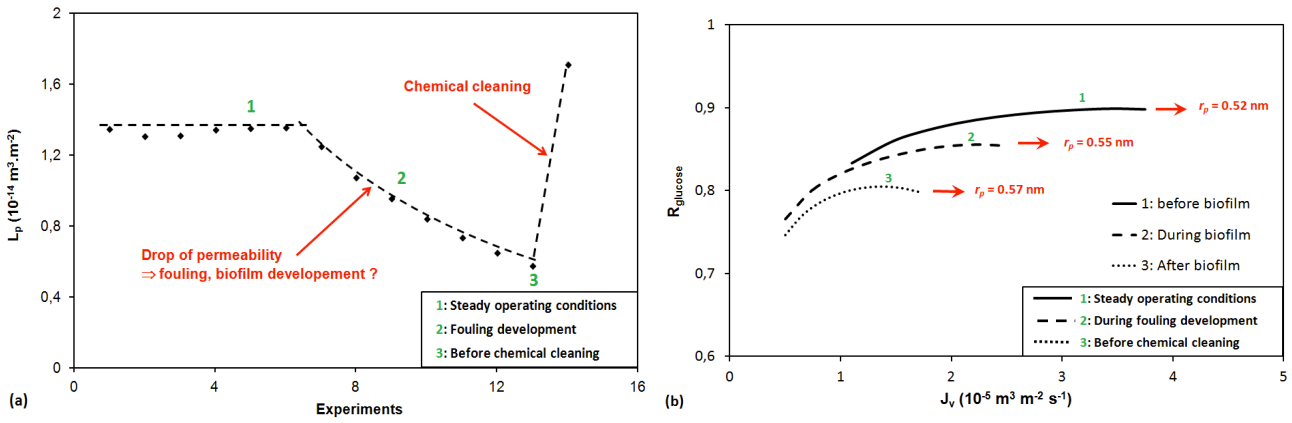

Figures 3: Evolution of experimental water permeability **(3a)** and glucose rejection **(3b)** during the biofilm development.

RESULTS & DISCUSSION

Membrane Water Permeability and Mean Pore Radius

Firstly, the hydrodynamic properties of the membrane were investigated in terms of water permeability L_p and mean pore radius r_p. Figures **3a** and **3b** show respectively evolutions of membrane permeability and glucose rejection (and thus pore radius), respectively in steady operating conditions (1), during the biofilm development (2) and before a chemical cleaning (3). From these figures, it can be seen that fouling had opposite influence on L_p and r_p. The latter indeed led to a decrease of L_p close to 50 %, whereas r_p increases of about 10% (see Table **1**). The permeability decrease was expected as fouling layer obviously induces an additional resistance, which leads to lower flux. Moreover, the biofilm can also partially clog pores and so reduce the surface available for the flow. Nevertheless, this pore obstruction is also supposed to lead to a decrease of the mean pore radius but the identified values show that the mean radius was increased by fouling. This observation can probably be explained by considering that the biofilm tends to obstruct preferentially the smallest pores and probably not the biggest ones, leading to an overall increase of the mean radius.

Experiments carried out after an acido-basic chemical cleaning (that destroyed biofilm) show that morphologic characteristics of the membrane were not identically restored, *i.e.* the water permeability and the mean pore radius obtained after cleaning (respectively 1.7 10^{-14} m^3 m^{-2} and 0.54 nm) were slightly higher than original ones.

Membrane Charge and Dielectric Constant within the Pores

Estimation of only structural data is not sufficient to characterize a membrane state and physico-chemical properties have also to be investigated. The model was also used to identify the dielectric constant of the solution within the pores ε_p and the volumetric membrane charge density X_d before and after the biofilm development. Two distinct identification procedures were applied for solutions of single salt or ternary mixtures. For single salt solutions, ε_p and X_d were assessed successively through assays in different conditions, whereas for salt mixtures both parameters were simultaneously identified from a single filtration.

Identification from Single NaCl Solutions:

With the first procedure, ε_p was estimated by simulating the rejection of a concentrated NaCl solution

Table 1: Model Parameters Assessed before and after the Biofilm Development

	Solutions	L_p (m^3 m^{-2})	r_p (nm)	ε_p	X_d (mol m^{-3})
Before biofilm	NaCl 400 mol m^{-3}	1.26 10^{-14}	0.52	59.5	~ 0
	NaCl 50 mol m^{-3}	1.30 10^{-14}	0.52	59.5	-115
After biofilm	NaCl 400 mol m^{-3}	0.59 10^{-14}	0.57	60	~ 0
	NaCl 50 mol m^{-3}	0.72 10^{-14}	0.57	60	-40

(400 mol m^{-3}), assuming that electrostatic interactions between ions and membrane charge are negligible at this concentration. In a second time, X_d was identified with a diluted NaCl solution (50 mol m^{-3}) by assuming that ε_p-value is independent of concentration. This method was carried out before and after the biofilm development and rejection curves (experimentally obtained and simulated with identified parameters) are shown in Figure **4**. The corresponding values of ε_p and X_d identified with these rejection curves are given in Table **1**.

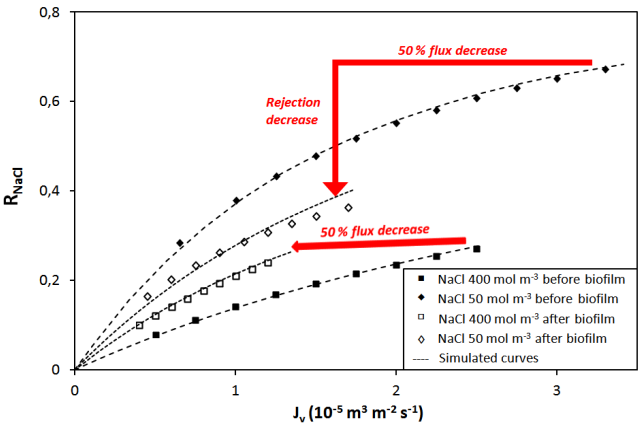

Figure 4: NaCl rejection curves used to estimate the values of ε_p and X_d before and after membrane deterioration {• experimental values and --- simulated curves obtained with identified parameters}.

The ε_p-values estimated with 400 mol m^{-3} NaCl solution were not affected by the presence of the biofilm (ε_p = 59.5 and 60). This observation is consistent with the assumption that biofilm has mainly modified the membrane surface but did not necessarily change significantly the properties of the pore inner solution. In contrast, it was found that the membrane charge was strongly influenced by the presence of biofilm. The biofilm has indeed screened the membrane charge, which was more or less three times lower than the native charge (in absolute value). This observation is in accordance with the decrease of rejection observed after biofilm development in Figure **4** for the NaCl 50 mol m^{-3} solution. For this reason, the difference between rejection curves of 50 and 400 mol m^{-3} solutions became really small after biofilm formation and the concentration had no longer a strong influence on the separation. Figure **4** also shows that rejection obtained with the 400 mol m^{-3} solution has slightly increased due to biofilm formation. However, it should be stressed that, even if rejection has increased at a given permeation flux, rejection measured at a given applied pressure was not significantly affected by the presence of biofilm, unlike permeation flux. Indeed, a strong flux decrease (50 %) induced by the biofilm formation was observed, regardless of the solution considered.

To conclude this part, results seem to indicate that only a diluted solution is required to characterize the evolution of the membrane charge by assuming that fouling or biofilm development does not affect the properties of the solution within the pores, and thus that ε_p is invariable for a given single salt.

Identification from NaCl / $MgCl_2$ mixtures

The previous method, based on the filtration of single salt (2 ions) solutions, requires a major assumption since it is supposed that the dielectric constant ε_p is constant irrespective of the concentration and equals to that estimated for a concentrated solution. This method has shown its limits and a second method based on the filtration of ternary mixtures (containing 3 ions) has therefore been developed to assess precisely ε_p and X_d values without additional assumption [16]. The latter, which consists in identifying ε_p and X_d simultaneously on multi-ionic mixtures, has shown a strong potential for the prediction of separation performances [17]. Indeed, with ternary mixtures, three rejection curves are obtained for each experiment instead of one in the case of single salt solutions. Hence, these three curves can be fitted simultaneously with only two parameters so that there is only one couple (ε_p, X_d) that correctly describes selectivity towards various ions. In this case, the obtained values are less controversial than those estimated from single salt solutions.

The membrane state was thus investigated before and after a storage period for a mixture containing 25 mol m^{-3} of NaCl and 12.5 mol m^{-3} of $MgCl_2$. Experimental and simulated rejection curves obtained in these conditions are provided in Figures **5a** and **5b** and the values of the various parameters are given in Table **2**.

First of all, it is worth noting that experimental rejection curves obtained for the three ions are correctly described by the model with the values presented in Table **2**. The couples (ε_p, X_d) identified before and after storage period seem to show that the membrane was only slightly modified during this period. The small variation observed on X_d could be interpreted by considering that the biofilm would have developed only at the external surface of the membrane but not inside pores, unlike filtration experiments with single NaCl solutions. Hence, fouling could have been partially destroyed by the water rinsing, which did not occur with the previous biofilm.

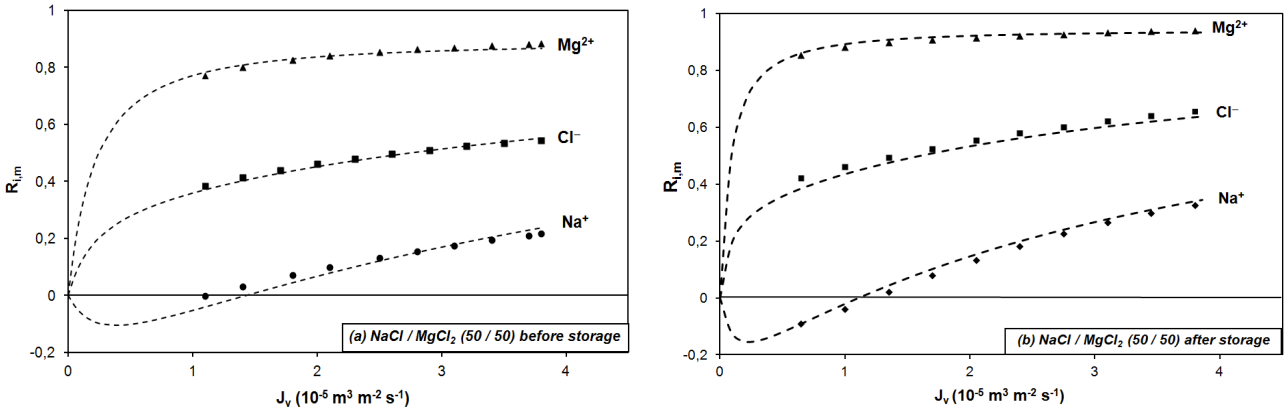

Figures 5: Rejection curves obtained for a NaCl / $MgCl_2$ mixture before storage **(5a)** and after one 1-year storage **(5b)**. {●, ■, ▲ experimental values and --- simulated curves obtained with identified parameters}.

Table 2: Model Parameters Assessed before and After the Storage

	L_p ($m^3\ m^{-2}$)	r_p (nm)	ε_p	X_d (mol m^{-3})
Before storage	$1.57\ 10^{-14}$	0.53	54.3	-10.4
After storage	$1.48\ 10^{-14}$	0.52	51.3	-6.6

This conclusion is in good agreement with the values of r_p and L_p estimated after the storage and water rinsing. Indeed, these values were found to slightly decrease after the storage but not as much as it was observed after the first biofilm formation, proving that no major modification of the pore surface occurred. Therefore, it seems that biofilm does not develop always in the same way and it would be interesting to investigate how operating conditions act on its formation. For instance, can the fact that biofilm was formed during a static storage period instead of filtration experiments does a matter?

It should be noticed that the X_d-values obtained with mixtures containing calcium are really low compared to those obtained with single NaCl solutions since divalent cations (calcium here) tend to screen more intensively the negative membrane charge compared to monovalent cations such as sodium. Hence, it is more difficult to observe the variation of membrane charge with solutions containing divalent cations and so it is also more complicated to detect a potential deterioration or fouling.

From earlier discussion, it appears that both procedures are complementary and the choice between them depends upon the purpose for which characterization is implemented. Indeed, adjustment of model parameters on ternary mixtures is more rigorous and should be used to accurately identify the membrane charge density and the dielectric constant inside pores without additional assumption. Moreover, it is worthwhile to note that values for single salt solutions can be extrapolated from those assessed with ternary mixtures as it was shown in a previous paper [17]. Conversely, adjustment on diluted NaCl solutions is the most suitable way to numerically characterize membrane state. Indeed, even if the identified membrane charge is arguable with this method, its high sensitivity to surface electrical modification and its easy processing make it perfectly adapted to follow-up state evolution. For industrial purpose, all the membrane characteristics could therefore be studied through a single filtration experiment containing a sugar for pore size estimation and a salt for surface charge estimation. It should be stressed that the salt has to be much diluted since it was also shown in previous studies that the presence of a salt acts on the size of the neutral solute and consequently, on the estimated pore size [18, 19].

CONCLUSION

This paper was devoted to the use of a knowledge model to characterize the physical state of a membrane. For this purpose, the impact of the development of a biofilm on the model parameters was investigated. Two identification procedures were described to characterize the influence of the membrane evolution on its charge density X_d and the properties of the solution within the pores ε_p.

It was found that the membrane fouling led to a decrease of the membrane permeability and an increase of the mean pore size, showing that mainly small pores are probably clogged by the biofilm. It was also shown that such a deposit screens the membrane charge but does not clearly modify the solvation properties of the solution within the pores. Such a model can thus be used to reveal a membrane drift along the time by means of one reference experiment (single salt or salts mixture) and also to check if the membrane has not too much changed after a specific event such as chemical cleaning. It was also shown in this paper that the best numerical way for membrane characterization is probably to identify physical model parameters from single NaCl filtrations because higher values of X_d lead to higher sensitivity to variation of surface charges. Indeed, the simultaneous identification of ε_p and X_d from mixtures leads to smaller X_d-values, which complicates the detection of membrane degradation. Finally, it was highlighted that a model can be a useful tool for diagnostic of used membranes in addition to direct characterization measurements such as streaming or membrane potentials [20, 21].

ACKNOWLEDGMENT

The authors would like to thank the Observatoire des Sciences de l'Univers THETA Franche-Comté-Bourgogne for its financial contribution.

NOMENCLATURE

A_k	=	porosity of the active layer
c_i	=	concentration of ion i within the pore (mol m^{-3})
$C_{i,p}$	=	permeate concentration of ion i (mol m^{-3})
$C_{i,r}$	=	bulk concentration of ion i (mol m^{-3})
$C_{i,w}$	=	wall concentration of ion i (mol m^{-3})
$D_{i,\infty}$	=	molecular diffusion coefficient of ion i at infinite dilution (m^2 s^{-1})
e	=	electronic charge (1.602177 10^{-19} C)
F	=	Faraday constant (96487 C mol^{-1})
j_i	=	ionic flux of ion i (mol m^{-2} s^{-1})
J_v	=	volumetric permeation flux (m^3 m^{-2} s^{-1})
k	=	Mass transfer coefficient (m s^{-1})
$K_{i,c}$	=	ionic hindrance factor for convection (dimensionless)
$K_{i,d}$	=	ionic hindrance factor for diffusion (dimensionless)
L_p	=	water permeability (m^3 m^{-2})
P	=	pressure (Pa)
R	=	universal gas constant (8.314 J mol^{-1} K^{-1})
r_i	=	Stokes radius of ion i (m)
$R_{i,m}$	=	real rejection of ion i (dimensionless)
$R_{i,obs}$	=	observed rejection of ion i (dimensionless)
r_p	=	average pore radius (m)
T	=	temperature (K)
U_t	=	Tangential velocity (m s^{-1})
V	=	solvent velocity (m s^{-1})
x	=	axial position within the pore (m)
X_d	=	effective membrane charge density (mol m^{-3})
z_i	=	valence of ion i (dimensionless)

Greek Symbols

$\gamma_{i,pore}$	=	activity coefficient of ion i in the pore side of the interface (dimensionless)
$\gamma_{i,sol}$	=	activity coefficient of ion i in the solution side of the interface (dimensionless)
ΔP	=	applied pressure (Pa)
ΔW_i	=	solvation energy barrier (J)
Δx	=	membrane thickness (m)
$\Delta\psi_D$	=	Donnan potential (V)
$\Delta\pi$	=	osmotic pressure difference (Pa)
ε_0	=	permittivity of free space (8.85419 10^{-19} C)
ε_b	=	bulk dielectric constant (dimensionless)
ε_p	=	pore dielectric constant (dimensionless)
η	=	dynamic viscosity (Pa s)
ϕ_i	=	steric partition coefficient (dimensionless)
ψ	=	electrical potential within the pore (V)

REFERENCES

[1] Pontié M, Lhassani A, Diawara CK, Elana A, Innocent C, Aureau D, *et al.*, Seawater nanofiltration for the elaboration of usable salty waters. Desalination 2004; 167: 347-355.

[2] Haddad R, Ferjani E, Roudesli MS, and Deratani A, Properties of cellulose acetate nanofiltration membranes. Application to brackish water desalination. Desalination 2004; 167: 403-409.

[3] Van Der Bruggen B, Vandecasteele C, Van Gestel T, Doyen W, and Leysen R, A review of pressure-driven membrane processes in wastewater treatment and drinking water production. Environ. Prog. 2003; 22(1): 46-56.

[4] Bourseau P, Vandanjon L, Jaouen P, Chaplain-Derouiniot M, Massé A, Guérard F, *et al.*, Fractionation of fish protein hydrolysates by ultrafiltration and nanofiltration: impact on peptidic populations. Desalination 2009; 244(1-3): 303-320.

[5] Brito Martínez M, Van der Bruggen B, Negrin ZR, and Luis Alconero P, Separation of a high-value pharmaceutical compound from waste ethanol by nanofiltration. J. Ind. Eng. Chem. 2012; 18(5): 1635-1641.

[6] Afonso MD and Bòrquez R, Nanofiltration of wastewaters from the fish meal industry. Desalination 2003; 151(2): 131-138.

[7] Van der Bruggen B, De Vreese I, and Vandecasteele C, Water reclamation in the textile industry: Nanofiltration of dye baths for wool dyeing. Ind. Eng. Chem. Res. 2001; 40(18): 3973-3978.

[8] Bowen WR and Welfoot JS, Modelling the performance of membrane nanofiltration-critical assessment and model development. Chem. Eng. Sci. 2002; 57(7): 1121-1137.

[9] Wang XL, Tsuru T, Nakao S, and Kimura S, The electrostatic and steric-hindrance model for the transport of charged solutes through nanofiltration membranes. J. Membr. Sci. 1997; 135: 19-32.

[10] Déon S, Dutournié P, and Bourseau P, Modeling nanofiltration with Nernst-Planck approach and polarization layer. AIChE J. 2007; 53(8): 1952-1969.

[11] Déon S, Dutournié P, Fievet P, Limousy L, and Bourseau P, Concentration polarization phenomenon during the nanofiltration of multi-ionic solutions: Influence of the filtrated solution and operating conditions. Water Res. 2013; 47(7): 2260-2272.

[12] Tsuru T, Nakao S, and Kimura S, Calculation of ion rejection by extended Nernst-Planck equation with charged reverse osmosis membranes for single and mixed electrolyte solutions. J. Chem. Eng. Jpn. 1991; 24: 511-517.

[13] Born M, Volumen and hydratationswärme der ionen. Z. Physik. Chem. 1920; 1(1): 45-48.

[14] Yaroshchuk AE, Dielectric exclusion of ions from membranes. Adv. Colloid Interface Sci. 2000; 85(2-3): 193-230.

[15] Van den Berg GB, Racz IG, and Smolders CA, Mass transfer coefficients in cross-flow ultrafiltration. J. Membr. Sci. 1989; 47(1-2): 25-51.

[16] Déon S, Dutournié P, Limousy L, and Bourseau P, Transport of salt mixtures through nanofiltration membranes: Numerical identification of electric and dielectric contributions. Sep. Purif. Technol. 2009; 69(3): 225-233.

[17] Déon S, Escoda A, Fievet P, Dutournié P, and Bourseau P, How to use a multi-ionic transport model to fully predict rejection of mineral salts by nanofiltration membranes. Chem. Eng. J. 2012; 189-190: 24-31.

[18] Boy V, Roux-de Balmann H, and Galier S, Relationship between volumetric properties and mass transfer through NF membrane for saccharide/electrolyte systems. J. Membr. Sci. 2012; 390–391(0): 254-262.

[19] Escoda A, Fievet P, Lakard S, Szymczyk A, and Déon S, Influence of salts on the rejection of polyethyleneglycol by an NF organic membrane: Pore swelling and salting-out effects. J. Membr. Sci. 2010; 347(1-2): 174-182.

[20] Pontié M, Chasseray X, Lemordant D, and Lainé JM, The streaming potential method for the caracterization of ultrafiltration organic membranes and the control of cleaning treatments. J. Membr. Sci. 1997; 129: 125-133.

[21] Lanteri Y, Fievet P, Magnenet C, Déon S, and Szymczyk A, Electrokinetic characterisation of particle deposits from streaming potential coupled with permeate flux measurements during dead-end filtration. J. Membr. Sci. 2011; 378(1-2): 224-232

Received on 09-07-2014 Accepted on 30-08-2014 Published on 05-12-2014